JBC RESEARCH ARTICLE

Role of omega-3 endocannabinoids in the modulation of T-cell activity in a multiple sclerosis experimental autoimmune encephalomyelitis (EAE) model

Received for publication, April 14, 2022, and in revised form, December 26, 2022 Published, Papers in Press, January 7, 2023,
https://doi.org/10.1016/j.jbc.2023.102886

Justin S. Kim[1,2,3], **Katiria Soto-Diaz**[4], **Tanner W. Bingham**[5], **Andrew J. Steelman**[2,4,6,7,*], **and Aditi Das**[1,2,3,5,6,*]

From the [1]*School of Chemistry and Biochemistry, Georgia Institute of Technology, Atlanta, Georgia, USA;* [2]*Division of Nutritional Sciences, and* [3]*Department of Comparative Biosciences, University of Illinois at Urbana-Champaign, Urbana, Illinois, USA;* [4]*Neuroscience Program, Beckman Institute, University of Illinois at Urbana-Champaign, Urbana, Illinois, USA;* [5]*Department of Chemistry, University of Illinois at Urbana-Champaign, Urbana, Illinois, USA;* [6]*Carl R. Woese Institute for Genomic Biology, and* [7]*Department of Bioengineering, Cancer Center at Illinois, Beckman Institute for Advanced Science and Technology, University of Illinois at Urbana-Champaign, Urbana, Illinois, USA*

Edited by Peter Cresswell

Epidemiological studies show that omega-3 fatty acid consumption is associated with improved conditions in neurodegenerative diseases such as multiple sclerosis (MS). However, the mechanism of this association is not well understood. Emerging evidence suggests that parent molecules such as docosahexaenoic acid are converted into downstream metabolites that are capable of directly modulating immune responses. *In vitro*, we found that docosahexaenoyl ethanolamide (DHEA), another dietary component and its epoxide metabolite, reduced the polarization of naïve T-cells toward proinflammatory Th1 and Th17 phenotypes. Furthermore, we identified that DHEA and related endocannabinoids are changing during the disease progression in mice undergoing relapse-remitting experimental autoimmune encephalomyelitis (RR-EAE). In addition, daily administration of DHEA to mice delayed the onset of disease, the rate of relapse, and the severity of clinical scores at relapse in RR-EAE, an animal model of MS. Collectively, these data indicate that DHEA and their downstream metabolites reduce the disease severity in the RR-EAE model of MS and can be potential dietary adjuvants to existing MS therapeutics.

Lipid mediators contribute to inflammation resolution following an inflammatory challenge (1, 2). There has been growing interest in unveiling the mechanisms by which nutritional status influences the immune response, especially related to the consumption of omega-3 fatty acids. Epidemiological studies correlated dietary intake of omega-3 fatty acids such as docosahexaenoic acid (DHA) with improved disease outcomes, including asthma, diabetes, and neurodegenerative diseases such as multiple sclerosis (MS) (3, 4). Consequently, there is strong interest in unveiling the changes in the DHA metabolome in the body following an enzymatic transformation of DHA into bioactive DHA derivatives. Previously, it was shown that DHA is converted into docosahexaenoyl ethanolamide (DHEA). DHEA, an analog of omega-6-derived endocannabinoid (eCB) anandamide (AEA) (5–9), is also known as synaptamide, which plays an important role in promoting synaptogenesis and is found endogenously in the brain and retina (9–13). Previous studies have demonstrated the ability of DHEA to attenuate lipopolysaccharide-induced activation of microglia (14, 15). Notably, a study focusing on bacterial and viral meningitis demonstrated that DHEA was reduced in the cerebrospinal fluid samples obtained from patients with neuroinflammation (16). Within the central nervous system (CNS), DHEA prevented neuropathic pain after spinal cord injury by suppressing spinal microgliosis (17). DHEA also influenced inflammatory markers and attenuated macrophage activation in adipocytes (18–20), indicating its potential influence on the peripheral immune system.

DHEA is a polyunsaturated lipid that can be metabolized by eicosanoid-synthesizing enzymes such as the cyclooxygenase, lipoxygenase, or cytochrome P450 epoxygenase enzymes to form oxidized metabolites. It was previously reported that DHEA is converted by lipoxygenase to form 10,17-dihydroxydocosahexaenoyl ethanolamide and 15-hydroxy-16(17)-epoxy-docosapentaenoyl ethanolamide that reduced the migration of polymorphonuclear leukocyte chemotaxis (21). In 2017, we demonstrated that cytochrome P450 enzymes can convert DHEA into DHEA-epoxides (epoxydocosahexaenoyl-ethanolamide [EDP-EA]) (22). One of the regioisomers, 19,20-EDP-EA, significantly reduced proinflammatory markers interleukin 6 (IL-6) and nitric oxide production, while promoting anti-inflammatory marker IL-10 in microglia (22). Overall, DHEA is further metabolized to downstream oxidized metabolites that are immunomodulatory and may be beneficial as a potential nutrition-based intervention in diseases with aberrant inflammatory responses such as MS.

MS is a chronic inflammatory, demyelinating, and debilitating disease of the CNS in which 85% of patients manifested a relapsing-remitting MS form where they experience episodic neurological dysfunction (relapses) followed by periods of

* For correspondence: Aditi Das, aditi.das@chemistry.gatech.edu; Andrew J. Steelman, asteelma@illinois.edu.

partial recovery (remission) (23, 24). While the natural history of MS is heterogeneous across patients (25–27), disease onset and exacerbation likely stems from an aberrant inflammatory response brought on by autoreactive T- and B-cells in the CNS parenchyma (28–30). In addition, several studies suggest that the inflammatory response and the subsequent axonal damage is exacerbated by responses including the production of proinflammatory molecules by activated microglia and infiltrating macrophages (31–33). Epidemiological studies suggest that omega-3-rich diets are associated with lower rates of MS (34) and possess beneficial anti-inflammatory (3, 35, 36) and neurological (37–39) health properties. A double-blind controlled trial in patients with relapse-remitting MS indicated a trend favoring those consuming an omega-3 supplementation over placebo pills (40). Another study showed that individuals consuming high omega-3 fatty acids through their diet reduced the risk of experiencing a clinical isolated syndrome (41). While there exists a correlation of improved quality of life in MS patients from increased omega-3 fatty acid intake, the precise mechanism is not well understood. Separately, studies utilizing phytocannabinoids Δ^9-tetrahydrocannabinol have been shown to reduce disease severity in experimental autoimmune encephalomyelitis (EAE) and Theiler's murine encephalomyelitis virus models of MS (42–46). Furthermore, cannabinoid treatment of MS patients decreased spasticity (47, 48), muscle stiffness (47, 49), and neuropathic pain (49). eCBs are derived from fatty acids and previous studies that showed that omega-6 eCBs such as AEA and 2-arachidonoylglycerol (2-AG) decrease inflammation through their interactions with cannabinoid receptors (50). As eCBs and cannabinoids interact with the same receptors (51), it is possible that DHEA and DHEA-epoxides that are DHA-based eCBs will be efficacious in ameliorating aberrant inflammatory diseases such as MS.

The goal of the current study is to show that DHEA reduces inflammatory responses while simultaneously inhibiting relapses and disease severity in a preclinical animal model of MS. The rationale of this study is based on the following observations: (A) eCBs modulate neuroinflammatory responses in MS, (B) phytocannabinoids from *Cannabis Sativa* and cannabinoid receptors play important role in MS, and (C) there is correlation of omega-3 fatty acid consumption with better quality of life in patients with MS. Overall, this demonstrates that DHEA, a dietary component also found endogenously in the human body, is dysregulated in EAE and influences the disease progression of relapse-remitting EAE (RR-EAE) animal model of MS. The fundamental understanding about eCB interactions with T-cells will help in the design of natural therapeutics in autoimmune diseases and will provide insight into understanding the mechanisms behind omega-3 consumption and conferred health benefits.

Results

eCBs inhibit T-cell polarization

Helper T-cells play an important role in MS pathogenesis and are essential for induction of EAE (52). Therefore, we measured the capacity of DHEA or DHEA-epoxide (eCB) and/or DHA-epoxide (non-eCB) to inhibit T-cell responses *in vitro* (Fig. 1*A*). Splenocytes were isolated from 2D2 mice, a T-cell receptor (TCR) transgenic mouse line in which 90% of helper T-cells bear a receptor specific for the myelin peptide antigen myelin oligodendrocyte glycoprotein $(MOG)_{35-55}$, preincubated with DHEA or DHEA-epoxide, and stimulated with antigen (Fig. 1*B*). Antigenic stimulation of 2D2 T-cells in this fashion promotes interferon gamma (IFNγ) production (53). Treatment with DHA-epoxide (19,20-) did not inhibit IFNγ production from antigen-stimulated cultures. However, both DHEA and DHEA-epoxide (19,20-) significantly reduced IFNγ production at high dose. Importantly, 10 μM DHEA-epoxide completely inhibited IFNγ production without inducing cell death as measured by lactate dehydrogenase production (Fig. 1*B*). It was previously shown that O-1966, a selective CB_2R agonist, can suppress T-cell proliferation and proinflammatory cytokine production (54) after stimulation with CD3 and CD28 crosslinking antibodies. To determine if DHEA can influence the polarization of naïve T-cells into proinflammatory Th1 or Th17 subsets, purified naïve T-cells were cultured under Th1 or Th17 polarizing conditions in the presence of DHEA or DHEA-epoxide (19,20-) (10 μM). After 48 h, the percentage of IFNγ- and IL17A-producing cells was determined by flow cytometry. Both DHEA and DHEA-epoxide treatment during the polarization phase reduced the percentage of Th1 and Th17 cells without altering viability (Fig. 1, *C–E*). Importantly, DHEA-epoxide treatment was more efficient at reducing Th17 polarization (Fig. 1*E*).

Central and peripheral levels of eCB levels in mice undergoing RR-EAE

eCB-mediated suppression of T-cell responses *in vitro* indicates that treatment may prove efficacious in the suppression of inflammatory diseases. AEA and 2-AG have been shown to change during neuroinflammation (55) and in a progressive model of EAE. We measured the levels of AEA, 2-AG, and DHEA eCBs at each stage of disease progression in RR-EAE. Throughout the course of the experiment, the associated weight change and clinical disability score of SJL/JC mice (N = 24, n = 6 per group) with EAE were measured (Fig. 2, *A* and *B*). Mice were sacrificed on day of immunization (day 0 p.i.), peak (day 14 p.i.), remission (day 19 p.i.), and at relapse (day 34 p.i.) time points of disease (Fig. 2*B*). Targeted LC–MS/MS analysis was used to analyze the levels of DHEA, AEA, and 2-AG to identify whether their levels change during disease progression. We report the levels of these three eCBs in the CNS (brain and spinal cord) and in the periphery (spleen).

In the spinal cord, DHEA was reduced at both peak and relapse time points compared with the baseline levels in RR-EAE mice. In addition, levels of omega-6-derived ethanolamide derivative AEA were reduced throughout the progression of disease (peak, remission, or relapse) compared with the baseline. In the brain, DHEA and AEA levels did not change during RR-EAE (Fig. 2*C*). However, 2-AG increased at

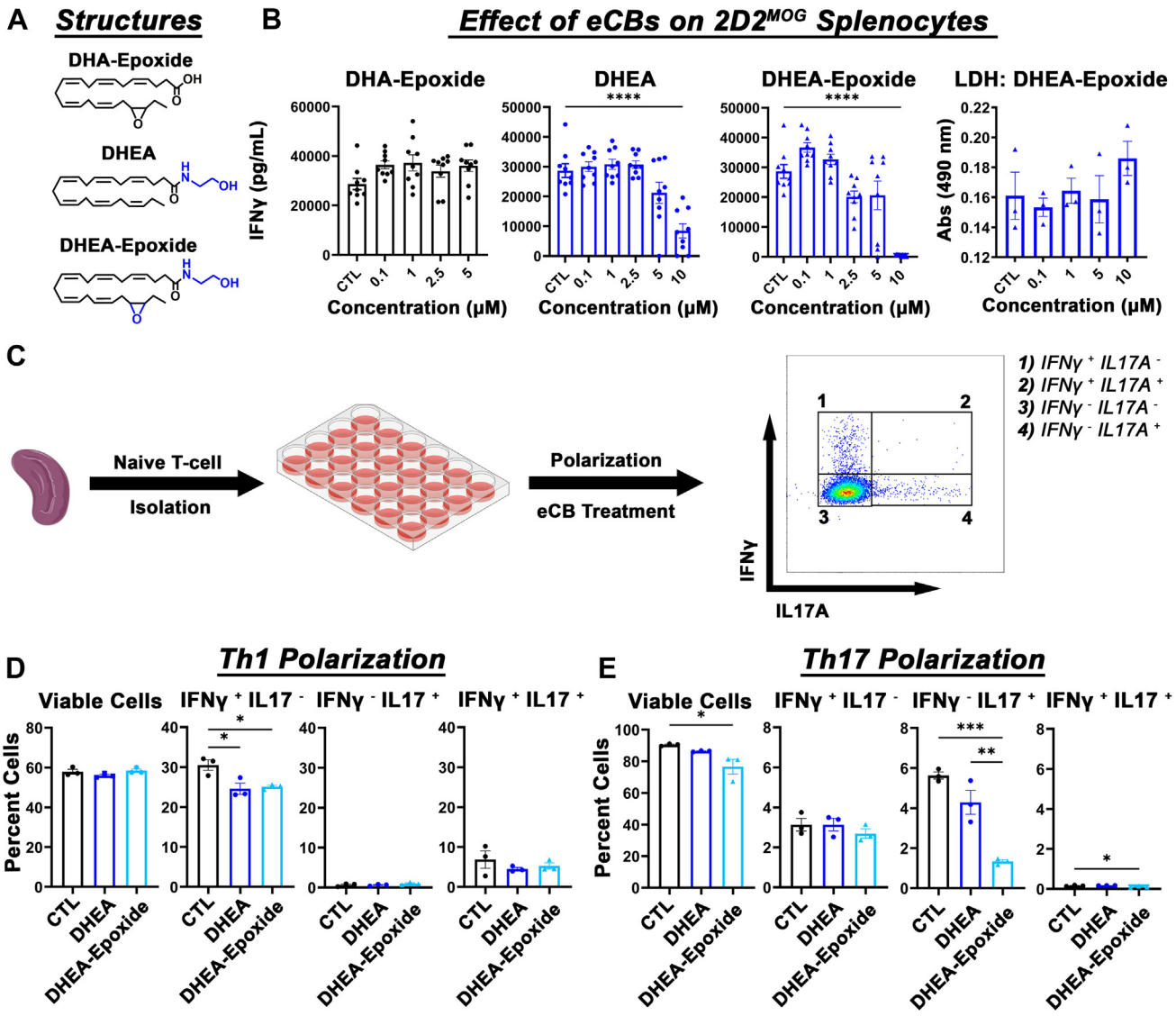

Figure 1. Endocannabinoids (eCBs) influence T-cells. *A*, structures of non-eCB epoxydocosahexaenoic acid (19,20-DHA-epoxide) and eCBs docosahexaenoyl ethanolamide (DHEA) and epoxydocosahexaenoyl ethanolamide (19,20-DHEA-epoxide). *B*, eCBs DHEA and DHEA-epoxide, but not non-eCB DHA-epoxide (19,20-), inhibits interferon gamma (IFNγ) production in TCR^{MOG} splenocytes without toxicity as measured by lactate dehydrogenase (LDH). For IFNγ measurements, there were n = 9 mice per treatment, obtained from three independent n = 3 mice per treatment experiments. The LDH assay is from n = 3 mice from one experiment. *C*, schematic of DHEA or DHEA-epoxide treatment on T-cell polarization to Th1 and Th17 and gating strategy. *D*, effects of eCB treatment during naïve T-cell to Th1 or (*E*) Th17 polarization. One-way ANOVA and Tukey's multiple comparisons test performed. MOG, myelin oligodendrocyte glycoprotein; TCR, T-cell receptor.

peak and relapse compared with baseline. During remission, 2-AG recovered to similar levels as the baseline. As eCBs influenced T-cells isolated from the spleen of the periphery (Fig. 1, *B–E*), we next investigated whether eCBs were changing in the spleen in the RR-EAE studies. DHEA levels were increased at remission and relapse compared with baseline. Similarly, AEA levels increased at remission compared with baseline and peak. While 2-AG levels increased at peak, there was recovery at remission and relapse (Fig. 2*D*). Interestingly, the changes in splenic levels of 2-AG were comparable to the brain. Overall, during the progression of the disease, the levels of the ethanolamine-modified fatty acids DHEA and AEA change significantly in the spinal cord and spleen but not in the brain.

DHEA treatment suppresses RR-EAE

To verify that 100 mg/kg/d DHEA maintains the baseline immune profile and is not toxic, we administered vehicle (saline containing 10% PEG 400 and 0.1% Tween-80) and DHEA daily to SJL/J mice in a nondisease state (Fig. S5). There were no differences of weight loss, behavioral, or clinical side effects in the DHEA treatment group compared with the vehicle control group. Since eCBs possess immunomodulatory properties, we next questioned whether DHEA treatment in healthy mice would alter the immune profile of the spleen. Treatment neither altered the percentage of viable or $CD4^+$ splenic cells in this organ (Fig. S5). Finally, there were no differences in eCB levels in the brain or spinal cord in a nondisease state (Fig. S5, *D* and *E*), suggesting that DHEA treatment in RR-EAE mice

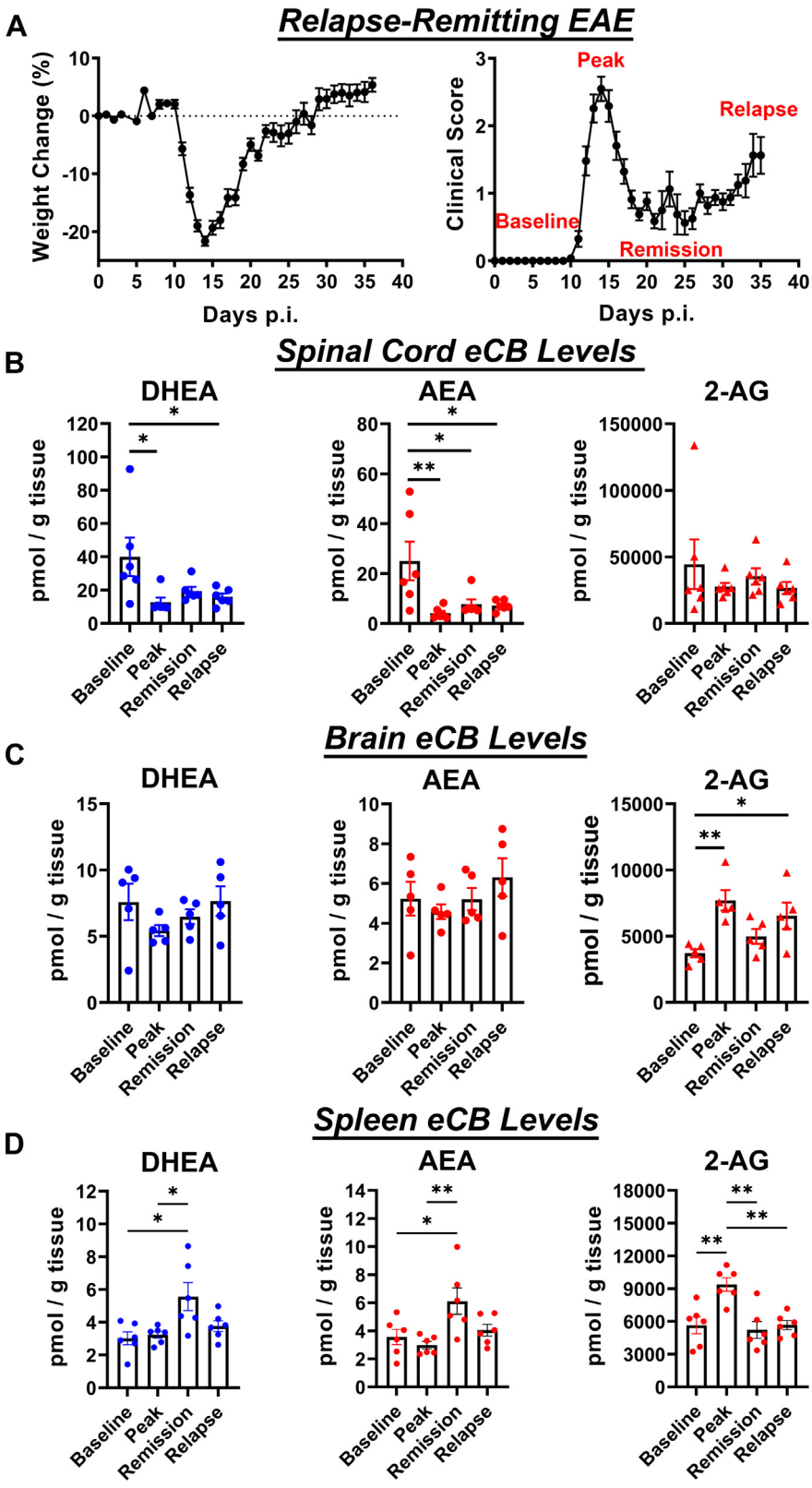

Figure 2. Endocannabinoid (eCB) system is dysregulated in EAE. *A*, EAE disease progression shown as clinical score and weight change (%) on immunized SJL/J mice (N = 40). Dysregulation of eCBs in the (*B*) spinal cord, (*C*), brain, or (*D*) spleen. eCBs docosahexaenoyl ethanolamide (DHEA), anandamide (AEA), and 2-arachidonoyl glycerol (2-AG) were detected and expressed as picomole/gram tissue. Tissues were harvested and analyzed as follows: baseline—day 0 p.i.; peak—day 14 p.i; remission—day 21 p.i.; relapse—day 35. n = 6 SJL/J mice per group were analyzed for statistical differences *via* one-way ANOV, and Tukey's multiple comparisons test was performed. EAE, experimental autoimmune encephalomyelitis.

likely influences the peripheral immune cells involved in EAE disease pathogenesis. Finally, fatty acid administration could lead to liver toxicity, but there were no effects of liver toxicity measured through serum analysis of liver metabolites (Fig. S6).

To determine if DHEA treatment could suppress EAE, we induced RR-EAE in SJL/J mice and treated the mice with either vehicle or a low dosage of DHEA (5 mg/kg/d). At this dose, we did not observe an effect of treatment on disease progression as determined by clinical score and weight change (Fig. S9 and Table S1). Thus, we next investigated the effects of DHEA at a higher and more relevant dosage of 100 mg/kg using the same RR-EAE model.

In this single-blinded experiment, there were three treatment groups (n = 12 per group) receiving vehicle ("vehicle"—*black*, saline containing 10% PEG 400, 0.1% Tween-80 beginning day 0), DHEA from day of immunization ("DHEA"—*blue*, beginning day 0), or DHEA after the peak disease ("DHEA postpeak"—*orange*, beginning day 19). Analysis of clinical scores indicated a delay of disease onset between the vehicle and DHEA (from day of immunization, *blue*) groups (Fig. 3, *A–C* and *H*). These data suggest that the DHEA treatment decreased the severity of the disease as compared with the vehicle group. Within the DHEA-treated group, there were responders and nonresponders to DHEA. We observe comparable disease progression of nonresponders to the vehicle control group, albeit with a slight delay of time to relapse by 3 days (Fig. S8). In the responders, we observed a delay in the time to disease onset but a greater disease severity at peak. The responders also exhibited a longer time to relapse from peak by approximately 18 days compared with 12 days in the vehicle group. To better visualize our observations, we plotted the data as percent of mice that were disease free (Fig. 3*G*). We observed that 40% of the mice in the DHEA group (*blue*, beginning day 0) develop disease at day 22 postimmunization compared with vehicle or the group receiving DHEA treatment after peak disease (*orange*, beginning day 19). Furthermore, these data revealed that the DHEA treatment group had a delay in the time to relapse compared with those in the vehicle control group (Fig. 3*H*). There was also a delay in time to relapse when DHEA was administered after the initial peak disease (postpeak; Fig. 2*I*). While there was no effect of time to relapse in mice administered DHEA from day of immunization, it is likely because DHEA initially delayed the day of onset in EAE mice (Fig. 3*I*). The summary of day of onset, maximum score, and cumulative scores between all three treatment groups is provided in Table S2.

Infiltrating CD4$^+$ cells in the CNS in RR-EAE mice treated with DHEA at 100 mg/kg body weight

Because CD4$^+$ T-cells play an imperative role in the pathogenesis of EAE, we questioned whether treatment affected their number or effector function within the CNS (Fig. 4). CD3 in the spinal cord was not detected. Therefore, cytokine productions on CD45^{hi} CD19$^-$ populations were examined. At days 48 and 49 postimmunization, there was a lower percentage of IFNγ$^+$IL17A$^-$ cells in the spinal cord from DHEA treatment beginning postpeak (Fig. 4*E*). While there were lower percentage and number of CD45^{hi}CD19$^-$ cells from treatment compared with vehicle, there was no effect. Considering the clinical disability scores of mice are observable after a change in immune response, it is likely that mice in the vehicle and DHEA group were undergoing remission and mice in the DHEA postpeak group were relapsing. Therefore, to get a better sense of how treatment affected CNS-infiltrating immune cells, we repeated the experiment and sacrificed mice just as the control group was beginning to relapse. We observed similar disease disability scores (Fig. 5*A*) and weight change (%) (Fig. 5*B*) in mice treated with either vehicle or DHEA (postpeak) as in our previous experiment (Fig. 3). DHEA (postpeak) treatment decreased the percentage of infiltrating IFNγ$^+$IL17A$^+$ cells in the brain (Fig. 5*D*). In the spinal cord, DHEA (postpeak) treatment reduced the percentage of IFNγ$^+$IL17A$^-$ producing cells (Fig. 5*F*).

Discussion

Omega-3 fatty acids are associated with anti-inflammatory (3, 35, 36) and neurological (37–39) health properties. Herein, we demonstrated that DHEA, derived from DHA, influences the polarization of Th1 and Th17 cells *in vitro*. As both Th1 and Th17 cells are suspected to have a pivotal role in disease progression of autoimmune diseases such as MS, we utilized RR-EAE to model the effects of DHEA on MS. We found that eCBs are dysregulated in the CNS during various disease stages, in a manner that was tissue dependent. Finally, we show that systemic DHEA treatment increased the time to relapse in RR-EAE mice, which was correlated to a reduction in CNS infiltrating IFNγ-producing Th1 cells, suggesting a promising natural diet–based therapeutic to help manage symptoms in MS patients.

Previously, it was shown that DHA-treated dendritic cells were poor stimulators of antigen-specific Th1 cell proliferation and differentiation (56), a process that would result in reduced IFNγ production by Th1 cells. Herein, we show that in isolated splenocytes from TCR^{MOG} mice, DHEA significantly reduced levels of IFNγ production, and DHEA-eepoxide abolished production of IFNγ. In contrast, DHA-epoxide did not decrease the IFNγ production, likely because it lacks the ethanolamide moiety and does not interact with cannabinoid receptors (22). As *Cnr2* has been shown to be expressed on T-cells (46) and cannabinoids can modulate Tcell responses (57), the ability of DHEA-derived molecules to act as cannabinoid receptor agonists is likely important for their immunomodulatory capacity. In addition to influencing TCR^{MOG} splenocyte response to its cognate self-antigen ($MOG_{35–55}$), we found that DHEA and DHEA-epoxide reduced T-cell polarization of both Th1 and Th17 cells. Finally, previous studies demonstrated that DHA and DHEA increase levels of IL-10 (22, 58), which can have a suppressive function on T-cells (58). While our study focuses on TCR^{MOG} splenocytes or isolated T-cells, it can be surmised that eCBs also influence other immune cells in the body leading to a synergistic immunomodulatory capacity. Indeed, we observed greater suppression by DHEA and DHEA-epoxides when we used

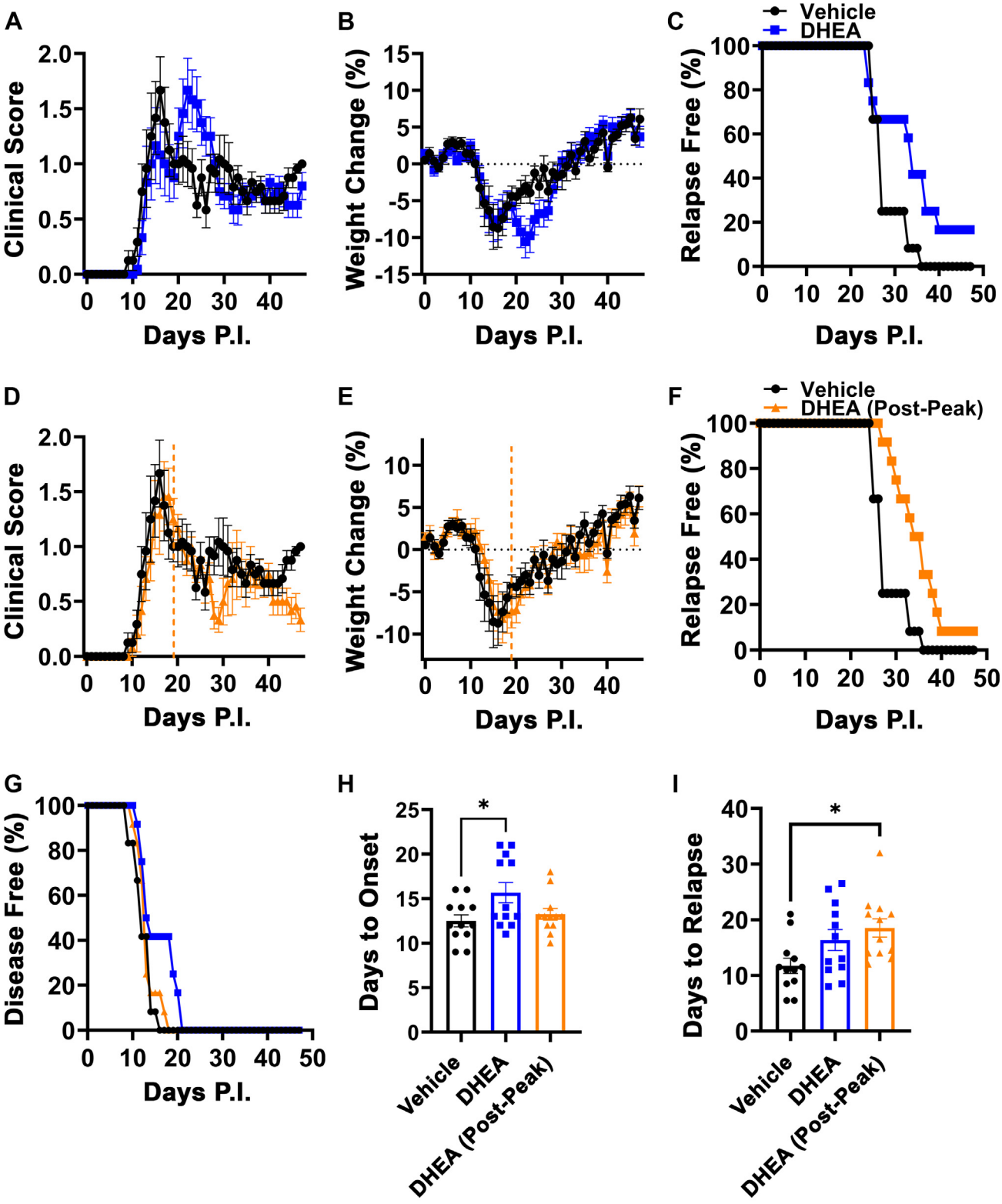

Figure 3. DHEA (100 mg/kg) treatment to EAE mice. SJL/J mice immunized with complete Freund's adjuvant containing $PLP_{131–159}$ (n = 12 per treatment group). *A*, clinical disability scores, (*B*) weight change (%) of immunized mice treated with vehicle (*black*, saline containing 0.1% Tween-80, 10% PEG 400), or DHEA beginning day of immunization (*blue*, 100 mg/kg body weight), and (*C*) percent relapse free. *D*, clinical disability scores, (*E*) weight change (%) and (*F*) percent relapse free of vehicle, or DHEA administered postpeak beginning on day 19 (*orange*, 100 mg/kg body weight). *G*, percent disease free from day of immunization, (*H*) average day of onset, and (*I*) time to relapse from day of peak disease for DHEA and DHEA postpeak compared with vehicle group. Analysis conducted by one-way ANOVA with Holm–Šidák multiple comparisons test. DHEA, docosahexaenoyl ethanolamide; EAE, experimental autoimmune encephalomyelitis; PLP, proteolipid protein.

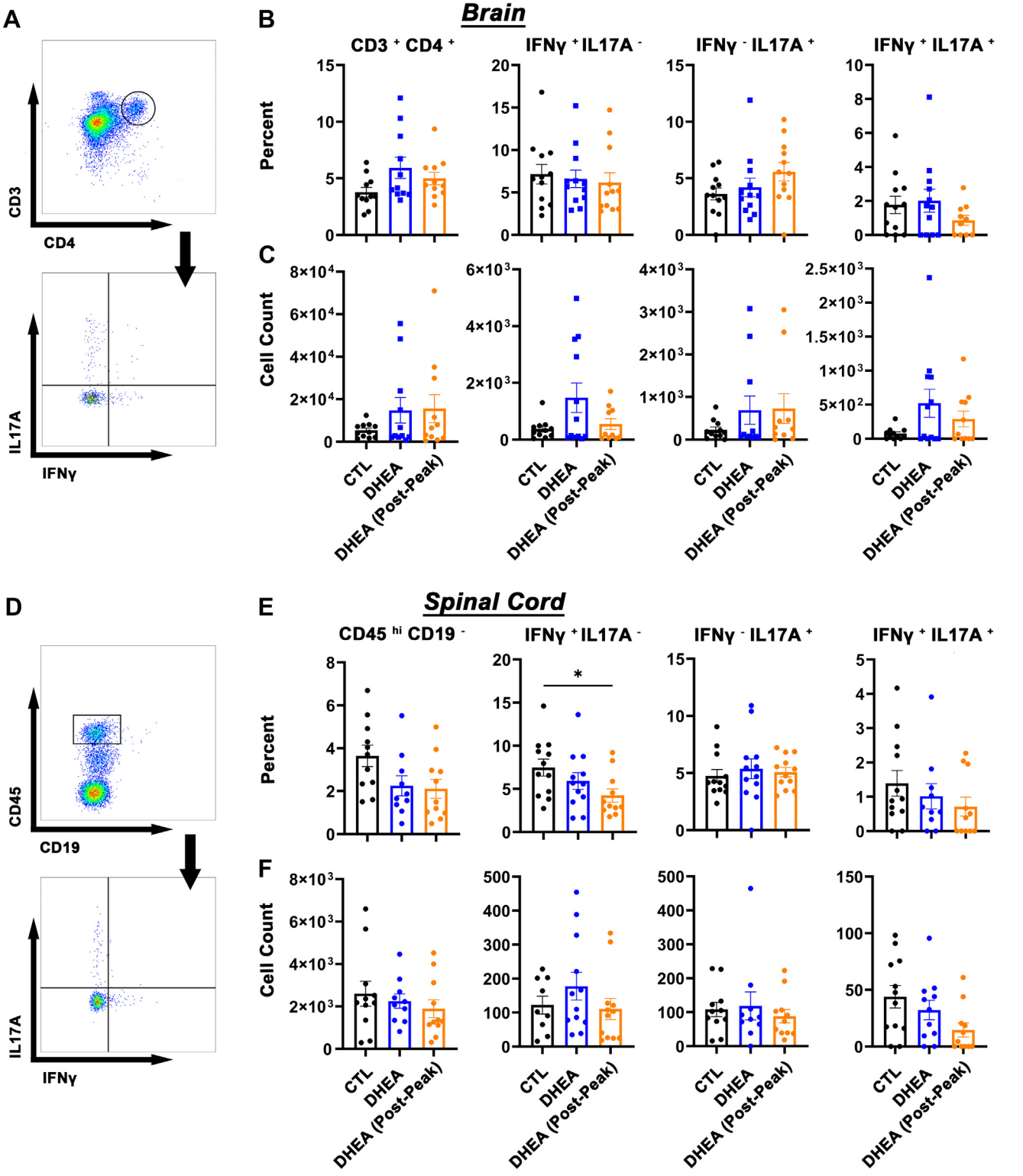

Figure 4. Infiltrating CD4$^+$ T-cells in CNS of DHEA-treated RR-EAE SJL/J mice. SJL/J mice immunized with complete Freund's adjuvant containing $PLP_{131–159}$ (n = 12 per treatment group). *A*, gating strategy for (*B*) percent and (*C*) number of $CD3^+CD4^+$, $IFNγ^+IL17A^-$, $IFNγ^-IL17A^+$, or $IFNγ^+IL17A^+$ T-cells in the brain. *D*, gating strategy for (*E*) percent and (*F*) number of infiltrating $CD45^{hi}CD19^-$, $IFNγ^+IL17A^-$, $IFNγ^-IL17A^+$, or $IFNγ^+IL17A^+$ T-cells in the spinal cord. Analysis conducted by one-way ANOVA with Holm–Šidák multiple comparisons test. CNS, central nervous system; DHEA, docosahexaenoyl ethanolamide; PLP, proteolipid protein; RR-EAE, relapse-remitting experimental autoimmune encephalomyelitis.

splenocyte cultures containing antigen-presenting cells including B-cells, macrophages, and dendritic cells than when we treated purified T-cell cultures.

Previously, it was shown that eCBs maintain homeostasis, and their dysregulation occurs in many chronic inflammatory diseases (59–61). Considering the epidemiological evidence that

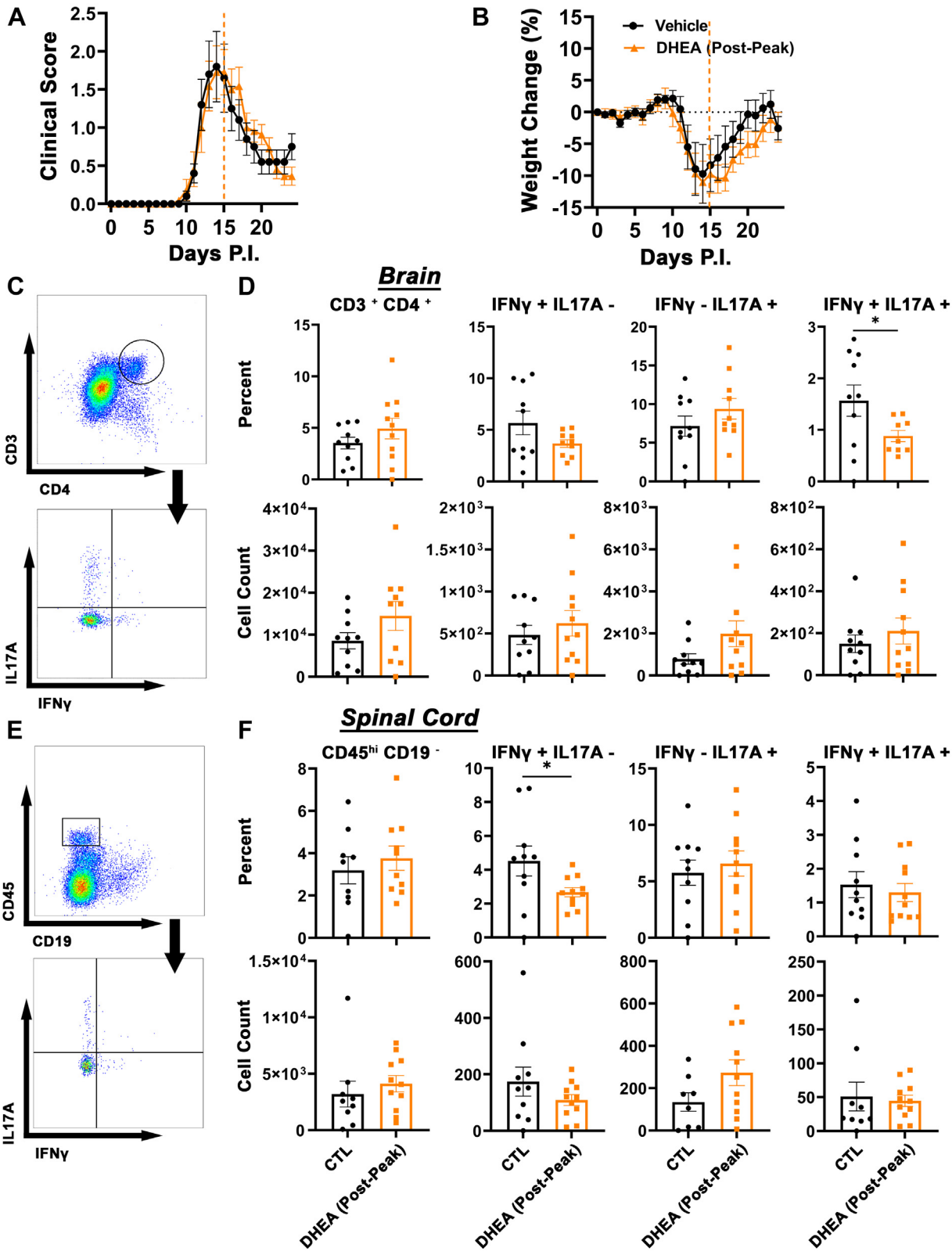

Figure 5. DHEA (postpeak)-treated RR-EAE mice beginning day 15. Tissues from SJL/J mice immunized with complete Freund's adjuvant containing $PLP_{131–159}$ (n = 10 for vehicle and n = 11 for DHEA) were collected at day 24 to identify infiltrating cells in the CNS. *A*, clinical disability score and (*B*) weight change (%) of RR-EAE mice treated with vehicle or DHEA (postpeak). *C*, gating strategy for (*D*) infiltrating $CD3^+CD4^+$, $IFN\gamma^+IL17A^-$, $IFN\gamma^-IL17A^+$, or $IFN\gamma^+IL17A^+$ T-cells in the brain. *E*, gating strategy for (*F*) infiltrating $CD45^{hi}CD19^-$, $IFN\gamma^+IL17A^-$, $IFN\gamma^-IL17A^+$, or $IFN\gamma^+IL17A^+$ T-cells in the brain. Analysis conducted by unpaired Student's *t* test. CNS, central nervous system; DHEA, docosahexaenoyl ethanolamide; PLP, proteolipid protein; RR-EAE, relapse-remitting experimental autoimmune encephalomyelitis.

support the beneficial effects of omega-3 fatty acids in persons with MS, we sought to determine whether eCBs (AEA, DHEA, and 2-AG) were dysregulated in an animal model of this disease. In mice undergoing RR-EAE, we observed a dysregulation of omega-3-derived DHEA as disease progressed. DHEA-epoxides however were unable to be quantified because of the limit of detection and low abundance at the whole tissue level. In addition, DHEA-epoxide is a dual moiety molecule containing both epoxide and ethanolamide moieties that are susceptible to metabolism, further contributing to the limitations of detection. 19,20-DHEA-epoxide can get metabolized into and accumulate as 19,20-dihydroxydocosapentaenoylethanolamide (19,20-DiHDPA-EA). In comparison to the baseline levels, they were reduced throughout disease progression, suggesting that its precursor (19,20-DHEA-epoxide) is also decreased (Fig. S15). In our study, we also observed a decrease in omega-6-derived AEA as disease progressed. This is contrary to another report where both AEA and 2-AG increased in striatum in a progressive model of MS (55). As omega-3 fatty acids are located throughout the brain and demyelination of white matter occurs in various regions, we investigated the whole tissue for an encompassing representation of eCB dysregulation. Another notable difference between our current study and those published previously is the type of disease being modeled. Progressive EAE models typically exhibit more neurodegeneration than relapsing-remitting models, which may affect eCB levels.

We further showed that the administration of DHEA to nondisease mice does not alter the eCB levels in the CNS (Fig. S5). Thus, the positive effects of DHEA treatment, including delay of disease onset and delay of relapse in our EAE studies, are likely a result of the effect on the peripheral immune system. While the mechanisms surrounding omega-3 fatty acid transport into the brain are still being studied, there are emerging data suggesting that fatty acid transporters including fatty acid–binding protein 5 (62, 63) or major facilitator superfamily domain–containing protein 2 (MFSD2A) (64, 65) at the blood–brain barrier play a critical role in this process. For instance, MFSD2A deficiencies resulted in hypomyelination (66), and MFSD2A knockout mice had reduced levels of DHA in the brain (63). Considering that MFSD2A is required for both fatty acid transport and myelination in the brain, it is likely that EAE also affects MFSD2A on endothelial cells at the blood–brain barrier, leading to reduced intake of fatty acids during a diseased state. Collectively, these data further strengthen the likelihood that DHEA treatment affects the peripheral immune system during RR-EAE. In addition, we show that DHEA administration to nondisease mice do not alter percentages of $CD4^+$ T-cells in the spleen. These data may indicate that overt activation is required to see an effect of DHEA treatment to splenic responses. In addition, it is plausible that DHEA treatment influences peripheral immune response and their infiltration into the CNS in a disease state but not in a healthy state. Alternatively, DHEA may affect their effector function rather than being cytotoxic, which is supported by the data presented herein. Hence, an increase of omega-3 consumption may be beneficial to patients diagnosed with MS and may alleviate symptoms of other autoimmune diseases.

In our RR-EAE mice study, we administered DHEA at either 5 mg/kg body weight or 100 mg/kg body weight. Importantly, treatments were administered *via* intraperitoneal injection on alternating lateral sides, a safe method for administering treatment (67). Furthermore, we selected to administer DHEA *via* intraperitoneal injection to first establish the systemic effects of eCB treatment as lipids can be altered through digestive processes within the gastrointestinal tract. When mice were treated with DHEA at a dose of 5 mg/kg body weight, we observed some positive trends (Fig. S9). Specifically, while there were no effects of DHEA treatment compared with vehicle, it appeared that DHEA reduced disease severity and time to relapse. We discovered that while there were positive trends, there were no differences in the infiltrating CD3+CD4+, or IL17-producing, IFNγ-producing, and IL10-producing T-cells. Importantly, we did observe any differences in IL4-producing T-cells (Figs. S9 and S10). One study describes that Food and Drug Administration–recommended dosage of omega-3 fatty acids are 3 g/day in chronic cardiovascular diseases (68). In previous double-blind omega-3 clinical trials, MS patients were administered 10 g omega-3 fatty acids a day (40). According to the Meeh–Rubner formula, a 75 kg human receiving only 40 mg/kg body weight omega-3 equates to approximately 160 mg/kg/day omega-3 in a 25 g mouse (69). Therefore, despite the considerably low administration of DHEA at 5 mg/kg body weight, our observations were promising and served as motivation for administering a higher dose. Indeed, we observed a delay of disease onset of mice treated with a higher dose (100 mg/kg body weight) of DHEA from day of immunization suggesting that DHEA is acting as an immunosuppressive molecule (70). In addition, DHEA was administered after peak (DHEA postpeak) to observe whether there was a delay in relapse or reduction of the relapse severity. We observed that in comparison to vehicle, DHEA administered postpeak delays the time to relapse and severity of the relapse. These data collectively suggest that DHEA is acting to suppress the immune response. Considering that RR-EAE is a $CD4^+$ T-cell-mediated process (71, 72), these *in vivo* data correspond with our findings that DHEA and DHEA-epoxide eCBs influence T-cell polarization, Th17 effector function, and antigen-specific activation in TCR^{MOG} splenocytes. Flow cytometry analysis did not indicate any differences in the IFNγ- or IL17—producing T-cells in the brain of our first study RR-EAE study (Fig. 4), which may be due to the stage of the disease progression when mice were sacrificed. At the time of sacrifice, the vehicle and DHEA groups were at their peak of relapse, whereas the DHEA postpeak group was at remission. Interestingly, we observed a decrease of $IL10^+$-producing cells within the $CD3^+CD4^+$ population. While clinical scores are indicative of disease progression, symptoms present itself after the immune response occurs within the body. As a result, the lack of differences in infiltrating inflammatory $CD4^+$ T-cells and decrease in $IL10^+$ cells in the brain from treatment may not be representative of the effects of DHEA (Fig. S11). In addition, we identified with CD45 and CD11b that there is a percent increase of lymphocytes and percent decrease of

microglia in the brain as a result of DHEA post-peak treatment (Fig. S12*B*). However, following normalization to the number of samples recovered prior to analysis *via* flow cytometry, there was no effect. While there is inflammation in the brain, the clinical disability outcomes observed in RR-EAE are due to lesions in the spinal cord. Therefore, changes of infiltrating cells in the spinal cord are of primary interest.

In the spinal cord of RR-EAE, SJL/JCrHsd mice treated with vehicle, DHEA beginning day of immunization and DHEA post-peak treatment, we observed a decrease of $IFN\gamma^{+}IL17A^{-}$ cells. While these cells may be indicative of overall cytokine production by cells present in the spinal cord, the precise cell types cannot be determined. It is plausible that in the spinal cord, there was a loss of CD3 and CD4 expression because of the activation of T-cells. Upon repeating DHEA (postpeak) treatment to RR-EAE mice, we observed a decrease in $IFN\gamma^{+}IL17A^{-}$ producing cells within the $CD45^{hi}CD19^{-}$ population. In addition, we observe a decrease in $FOXP3^{+}IL10^{+}$, $FOXP3^{+}IL10^{+}$, and $FOXP3^{-}IL10+$ cells in the brain. Disease progression and clinical disability are due to legions present in the spinal cord. Our observed effects may be due to the draining of $FOXP3^{+}$ cells from the brain into the spinal cord, which regulate polarized effector T-cells. Importantly however, we see an increase of T-regulatory cells (Fig. S13, *E* and *F*) in the spinal cord, the site of legions, and subsequent cause of clinical disability. Interestingly, we do not observe any effects of DHEA post-peak treatment on myeloid or microglia populations (Fig. S14). Nevertheless, these data align with our TCR^{MOG} and Th1 polarization data that DHEA and DHEA-epoxide treatment influence Th1 cells.

It is worthy to note that eCB treatment on RR-EAE mice is not limited to T-cells. While the SJL/JCrHsd RR-EAE model is a $CD4^{+}$ T-cell-mediated response, *in vivo* treatments are innately a more complex system than purified and isolated naïve T-cell cultures. It is plausible that there are also effects on antigen-presenting cells such as macrophages, B-cells, and dendritic cells. While the goal of this study was to study the effects of eCBs on T-cell activity, future studies investigating antigen-presenting cells would be worthwhile to pursue.

Modulation of the eCB system has been shown to affect the pathogenesis of EAE. For instance, CB_2 knockout mice had greater disease score in Ac1-11 peptide–induced immunization (73). In the same study, treatment with 25 mg/kg body weight tetrahydrocannabinol suppressed EAE in ABH Biozzi mice suggesting that cannabinoid receptor activation may ameliorate EAE (73). Another study showed that in C57BL/6 mice immunized with MOG_{35-55}, highly selective CB_2 agonist Gp1a administration reduced incidence of EAE by 60% and reduced the maximum score and total cumulative score over the course of 36 days (74). In our study, DHEA-epoxide (19,20-) was consistently more potent than DHEA at 10 μM *in vitro*. In cannabinoid receptor activation studies, DHEA had an EC_{50} value of 1044 nM for CB_1 compared with DHEA-epoxide (19,20-) of 108 nM (22). Similarly, DHEA-epoxide (19,20-) had greater affinity than DHEA for CB_2, where EC_{50} values were 280 and 305 nM, respectively (22). Considering that eCBs possess greater affinities for cannabinoid receptors, it is likely that the immunosuppressive capacity of DHEA-epoxide is a direct result of its ability to activate the cannabinoid receptors (75–77). Furthermore, while it is possible that DHEA is hydrolyzed into DHA, DHA is not an eCB as it does not activate the cannabinoid receptors. While current evidence suggests that this is a cannabinoid receptor–mediated process, further studies verifying this hypothesis are of interest in the future. Moreover, it is plausible that DHEA is hydrolyzed to DHA, which is then converted into other anti-inflammatory eicosanoids. For instance, resolvin D1, resolvin D2, and maresin 1 are non-eCB metabolites that inhibited secretion of IFNγ and IL-17 in human $CD4^{+}$ T-cells (78), processes that are involved in MS progression. Furthermore, there is dysregulated biosynthesis of these specialized proresolving lipid mediators derived from fatty acids such as omega-3 fatty acids in several diseases (79), including MS (80). Other specialized proresolving lipid mediators such as maresin 1 have been shown to ameliorate EAE (81) and promote inflammation resolution and recovery after a spinal cord injury (82).

In conclusion, this is the first study to demonstrate that downstream molecules of omega-3 fatty acid DHA can influence EAE progression by modulating the immune profiles. Importantly, this further illustrates the hypotheses that conversion of DHA into DHEA and further to DHEA-epoxides leads to the formation of potent molecules that are immunosuppressive. Overall, DHEA and other lipid metabolites can influence T-cell polarization and influence T-cell effector function, thereby showing a positive outcome in autoimmune diseases such as MS.

Experimental procedures

EAE experiments in animals

All animal care and experimental procedures were approved by the Institutional Animal Care and Use Committee at the University of Illinois Urbana-Champaign and were performed in accordance with the National Institutes of Health Guidelines for Care and Use of Laboratory Animals. Six- to 8-week-old female SJL/JCrHsd mice (Envigo no.: 052) were obtained from Envigo. All animals were housed under a reverse 12 h light/dark cycle with food (Teklad 2918) and water ad libitum. One week prior to induction of RR-EAE, mice were stratified by weight and housed four per cage. Mice were treated daily with vehicle or DHEA (0.5 mg/kg/day) beginning on the first day of immunization. Treatments were administered *via* intraperitoneal injection on alternating lateral sides. C57BL/6 mice (age 9–12 weeks) were utilized for T-cell polarization experiments, and C57BL/6-Tg(Tcra2D2, Tcrb2D2)1Kuch/J mice were utilized for primary splenocyte cultures.

Induction of RR-EAE

RR-EAE was induced by subcutaneous injection of complete Freund's adjuvant (CFA) and proteolipid protein $(PLP)_{139-151}$ emulsion on 9-week-old mice. CFA was prepared by mixing incomplete Freund's adjuvant (Sigma–Aldrich; catalog no.: F5506) and inactivated *Mycobacterium tuberculosis* H37 RA (Difco; catalog no.: 231141) at a concentration of 4 mg/ml.

$PLP_{139–151}$ (AS-63912; Anaspec, Inc) was solubilized in PBS (pH 7.4) at a concentration of 1.5 mg/ml. Equivalent volumes of $PLP_{139–151}$ and CFA were mixed in a dropwise manner while vortexing between each drop. The $PLP_{139–151}$ and CFA emulsion was then vortexed for 1 h. Mice were anesthetized with 4% isoflurane and then subcutaneously injected with 100 μl $PLP_{131–151}$ and CFA emulsion distributed equally over two spots across the flank. Each mouse received a total of 200 μg *M. tuberculosis* and 75 μg $PLP_{139–151}$. Mice were weighed and monitored daily for clinical disability in a blinded manner.

Clinical scoring of RR-EAE

Active RR-EAE was scored as previously described (83) with slight modification. Clinical score severity was assessed on a scale of 0 to 5 utilizing the following scoring system: 0, normal mouse with no signs of disease; 0.5, tail weakness or hindlimb weakness; 1, tail paralysis or tail weakness and hindlimb weakness; 1.5, tail paralysis and hindlimb weakness; 2, tail paralysis, loss of righting reflex, and hindlimb weakness; 2.5, partial hindlimb paresis; 3, one complete limb paralysis; 3.5, one complete limb paralysis and weakness in the other limb; 4, two limb paralysis; 4.5, two limb paralysis and weakness in forelimb; 5, moribund state/death by EAE. All atypical symptoms were also monitored. To be considered a relapse, a corresponding 5% body weight loss and decreased clinical score of 0.5 was required.

Tissue harvesting

Mice were asphyxiated with CO_2, right atrium cut, and blood collected. Mice were then perfused with 30 ml of sterile 1× PBS at a rate of 1 ml/min. Blood was processed for serum and stored for later analysis. Brain, spinal cord, and spleens were collected under sterile conditions in RPMI1640 and stored on ice for culturing. Tissues collected for eCB extraction were collected in a preweighed cryovial and flash frozen in liquid nitrogen for analysis.

eCB extractions

All extractions were completed on ice using solvent extraction systems with volumes relative to tissue mass. Briefly, 9:1 ethyl acetate:hexane supplemented with *N*-[1-(1-oxopropyl)-4-piperidinyl]-*N*′-[4-(trifluoromethoxy)phenyl]-urea (10 μM; Cayman Chemical; catalog no.: 11120) and PMSF (1 mM; Gold Bio; catalog no.: P-470) were utilized in a 1:20 tissue mass (g):volume (ml) ratio. Tissues with homogenized with a biohomogenizer for 30 s on ice, and 9:1 ethyl acetate:hexane and distilled water containing *N*-[1-(1-oxopropyl)-4-piperidinyl]-*N*′-[4-(trifluoromethoxy)phenyl]-urea and PMSF were added. The contents were then vortexed and subsequently centrifuged at 800*g* for 5 min. The upper organic layer was collected, dried under continuous stream of nitrogen gas, and eCB quantification conducted.

Quantification of eCBs

Samples were analyzed with the 5500 QTRAP LC/MS/MS system (Sciex) in Metabolomics Lab of Roy J. Carver Biotechnology Center, University of Illinois at Urbana-Champaign. Software Analyst 1.7.1 (Sciex) was used for data acquisition and analysis. The 1200 series HPLC system (Agilent Technologies) includes a degasser, an autosampler, and a binary pump. The LC separation was performed on an Agilent Eclipse XDB-C18 (4.6 × 150 mm, 5 μm) with mobile phase A (0.1% formic acid in water) and mobile phase B (0.1% formic acid in acetonitrile [ACN]). The flow rate was 0.4 ml/min. The linear gradient was as follows: 0 to 2 min, 90% A; 10 min, 5% A; 23 to 30 min, 0% A; and 30.1 to 37 min, 90% A. The autosampler was set at 10 °C. The injection volume was 10 μl. Separation chromatograms can be viewed in Fig. S3. Mass spectra were acquired under both positive (ion spray voltage was +5500 V) and negative (ion spray voltage was −4500 V) electrospray ionization (ESI). The source temperature was 450 °C. The curtain gas, ion source gas 1, and ion source gas 2 were 32, 50, and 55, respectively. Multiple reaction monitoring was used for quantitation: in the positive mode, AEA *m/z* 348.3 → *m/z* 62.1; 2-AG *m/z* 379.2 → *m/z* 79.0; EPEA *m/z* 346.3 → *m/z* 62.1; DHEA *m/z* 372.4 → *m/z* 62.1; DHG *m/z* 403.1 → *m/z* 119.0; 19/20-EDP-EA *m/z* 388.1 → *m/z* 62.1; and 19/20-DiHDPA-EA *m/z* 406.3 → *m/z* 388.3. In the negative mode, 19/20-EDP *m/z* 343.2 → *m/z* 281.2; 19/20-DiHDPA *m/z* 361.1 → *m/z* 273.1. Internal standard d4-AEA was monitored at *m/z* 352.3 → *m/z* 287.2 (positive ESI), and d5-DHA was monitored at *m/z* 332.2 → *m/z* 288.2 (negative ESI).

Liver toxicity

Female SJL/JCrHsd (n = 6 per group) were treated with 100 mg/kg/day DHEA *via* intraperitoneal injection for 33 days. Mice were euthanized, and tissues were collected. The blood was collected without anticoagulants and centrifuged at 1000*g* for 5 min at 4 °C. The serum was isolated and immediately frozen. Samples (200 μl each) were pooled (n = 3) and submitted to the Veterinary Diagnostic Laboratory at the University of Illinois at Urbana-Champaign for liver chemistry profile analysis of alanine transaminase, alkaline phosphatase, gamma glutamyltransferase, total bili, blood urea nitrogen, glucose, albumin, and cholesterol.

Primary cell isolation

Tissues were placed on a 70 μm cell strainer and mashed with a sterile plunger. Red blood cells were lysed using 1× red blood cell lysis buffer and subsequently inhibited with equal volume of RPMI1640. Following centrifugation at 400*g* for 5 min and removal of supernatant, single-cell suspensions were created in RPMI1640 containing 10% fetal bovine serum (FBS), 1× Glutamax, 1 mM sodium pyruvate, and 100 U/ml penicillin/streptomycin. About 5×10^5 cells/well were plated in 96-well plate prior to treatments and stimulation. For analysis of infiltrating cells in the CNS, brains and spinal cords were mashed, cells dissociated with Accutase (Thermo Fisher; catalog no.: A1110501) for 30 min at 37 °C, and filtered through a 70 μm cell strainer. Cells were resuspended in 30% Percoll (Thermo Fisher; catalog no.: 45-001-747), and an

underlayer of 70% Percoll was added. Cells were spun at 20,000*g* for 1 h, and the middle interface was collected.

2D2^{MOG} primary splenocyte cultures

C57BL/6-Tg(Tcra2D2, Tcrb2D2)1Kuch/J mice were utilized for primary splenocyte cultures. Spleens were isolated and processed as described in the aforeemntioned *Primary cell isolation* methods section. Splenocytes were plated in 96-well plate at 5 × 10^5 cells/well. Splenocytes were pre-incubated with 10 μM DHEA or DHEA-epoxide (19,20-) for 30 min and then stimulated with 25 μg/ml MOG_{35-55}. Following a 48 h stimulation, cells were spun for 5 min at 700*g*, and supernatants were collected for cytokine analysis. DHEA and DHEA-epoxide (19,20-) were in 100% pure ethanol solution, and final concentrations of ethanol in cell cultures were 0.01%.

Naïve T-cell isolation and polarization

Naïve $CD4^+$ T-cells (Thermo Fisher; catalog no.: 8804-6824-74) were isolated and then polarized into Th1 cells (R&D Systems; catalog no.: CDK018). Th17 cells were obtained using the same naïve $CD4^+$ T-cell isolation kit but polarized to Th17 (R&D Systems; catalog no.: CDK017). Medium used was X-VIVO 15 hematopoietic cell media (Lonza; catalog no.: BE02-060Q) supplemented with 10% FBS and 100 U/ml penicillin/streptomycin. Following polarization to Th1, cells were pre-treated for 30 min with eCBs prior to stimulation. Cells were stimulated with phorbol 12-myristate 13-acetate and ionomycin (0.081 and 1.34 μM, respectively), and brefeldin A added. Following a 4 h incubation in 37 °C, cells were harvested and processed for flow cytometry as described later.

Flow cytometry and antibodies

Following treatment, cells were resuspended in flow buffer (2% FBS in 1× PBS), and cell surface marker antibodies were added. Following a 15 min incubation at 4 °C in the dark, cells were washed twice and prepared for intracellular cytokine staining. Cells were fixed in intracellular fixation buffer (eBioscience; catalog no.: 00-8222-49) for 20 min at room temperature, followed by 10 min incubation in permeabilization buffer (eBiosciences; catalog no.: 00-8333-56). Cells were then resuspended in permeabilization buffer and incubated with intracellular antibodies for 20 min in the dark at room temperature. Cells were washed twice and analyzed on the Invitrogen Attune NxT flow cytometer. Compensations were conducted using UltraComp eBeads (Invitrogen; catalog no.: 01-2222). Antibodies used were as follows; IFNγ (rat anti-mouse, PE-Cyanine7, Clone XMG1.2, eBioscience; Fisher Scientific, catalog no.: 50-156-14), FOXP3 (rat antimouse, FITC, Clone FJK-16s, eBioscience, Fisher Scientific, catalog no.: 50-112-9051), IL-10 (rat antimouse, APC, Clone JES5-16E3, eBioscience, Fisher Scientific, catalog no.: 50-122-3185), IL-17A (rat antimouse, FITC, Clone eBio17B7, eBioscience, Fisher Scientific, catalog no.: 50-112-9414), IL-4 (rat antimouse, APC, Clone 11B11, eBioscience, Fisher Scientific, catalog no.: 5015301), CD3 (rat antimouse, Alexa Fluor 700, Clone 17A2, eBioscience, Fisher Scientific, catalog no.: 50-168-42), and CD4 (rat antimouse, APC-Cy7, Clone RM4-5, BioLegend, catalog no.: 100526).

Chemical synthesis of DHEA

For primary cultures and EAE experiments, DHEA (Cayman Chemical; catalog no.: 10007534) was utilized. Molecules were checked *via* ESI mass spectrometry in positive ion mode as seen in Fig. S4. For DHEA treatments to nondisease mice, chemical syntheses were performed, and analysis was conducted as follows. Unless otherwise noted, all reactions were carried out under an ambient atmosphere. All chemicals were purchased from commercial suppliers and used as received. Dry dichloromethane (DCM; CH_2Cl_2) was obtained by passing commercially available anhydrous oxygen-free HPLC-grade solvents through activated alumina columns. Analytical TLC was performed on Merck silica gel 60 F254 glass plates. Visualization was accomplished with UV light and/or potassium permanganate. Retention factor (R_f) values reported were measured using a 5 × 2 cm TLC plate in a developing chamber containing the solvent system described. Flash column chromatography was performed using Silicycle SiliaFlash P60 (C18-functionalized SiO_2, 40–63 μm particle size, 230–400 mesh). ^1H and ^{13}C NMR spectra were recorded on Bruker 500 (500 MHz, ^1H; 126 MHz, ^{13}C) or Varian Unity Inova 500 (500 MHz, ^1H) spectrometers. Spectra are referenced to residual chloroform (δ = 7.26 ppm, ^1H; 77.16 ppm, ^{13}C). Chemical shifts are reported in parts per million (ppm). Multiplicities are indicated by s (singlet), d (doublet), t (triplet), q (quartet), m (multiplet), and br (broad). Coupling constants J are reported in hertz (Hz). Mass spectrometry was performed by the University of Illinois Mass Spectrometry Laboratory. ESI+ spectra were performed using a time-of-flight (TOF) mass analyzer. Data are reported in the form of *m/z* (intensity relative to the base peak = 100). Infrared spectra were measured neat on a PerkinElmer spectrum BX FT-IR spectrometer. Peaks are reported in cm^{-1} with indicated relative intensities: s (strong, 0–33% T); m (medium, 34–66% T), w (weak, 67–100% T), and br (broad).

To a mixture of 1-ethyl-3-(3-dimethylaminopropyl)carbodiimide (233 mg, 1.22 mmol, 2 equivalents), *N*-hydroxyphthalamide (109 mg, 670 μmol, 1.1 equivalents) and 4-dimethylaminopyridine (7.45 mg, 60.8 μmol, 0.1 equivalents) in DCM (6.0 ml) was added DHA (200 mg, 608 μmol, 1 equivalent). The mixture was stirred for 3 h, and the solvents were removed *in vacuo*. Hexanes (20 ml) were then added, and the resulting suspension was filtered through a pad of silica. The silica was then washed with another 40 ml hexanes to make sure all the product was washed off the silica. The filtrate was then concentrated, and THF (12 ml) was then added. To this solution was added K_2CO_3 (168 mg, 1.22 mmol, 2 equivalents), H_2O (12 ml), and ethanolamide (74.5 mg, 1.22 mmol, 2 equivalents). The resulting mixture was stirred for 3 h, and then the reaction was diluted with 1 M HCl (12 ml) and CH_2Cl_2 (30 ml). The layers were separated, and the aqueous phase was extracted with CH_2Cl_2

(2 × 30 ml), and the combined organic extracts were washed with brine (50 ml), dried over $MgSO_4$, filtered, and concentrated under reduced pressure. The residue was purified by flash chromatography (C18-functionalized SiO_2, H_2O:MeCN = 3:1 → 1:3) to yield a yellow oil (211 mg, 510 μmol, 84%). These molecules were verified through ^1H NMR and ^{13}C NMR as seen in Fig. S7.

R_f = 0.30 (SiO_2, CH_2Cl_2:MeOH = 16:1)

^1H NMR (500 MHz, $CDCl_3$) δ 5.93 (s, 1H), 5.48-5.25 (m, 12H), 3.72 (t, J = 5.3 Hz, 2H), 3.42 (q, J = 5.3 Hz, 2H), 2.93-2.76 (m, 10H), 2.62 (s, 1H), 2.46-2.38 (m, 2H), 2.27 (t, J = 8.0 Hz, 2H), 2.07 (p, J = 7.5, Hz, 2H), 0.97 (t, J = 7.5 Hz, 3H).

^{13}C NMR (126 MHz, $CDCl_3$) δ 173.8, 132.2, 129.7, 128.7, 128.5, 128.44, 128.42, 128.23, 128.21, 128.20, 128.1, 128.0, 127.2, 62.7, 42.6, 36.5, 25.80 (2 overlapping peaks), 25.78, 25.76, 25.69, 23.5, 20.7, 14.4.

HRMS (ESI-TOF, *m/z*) calculated for $C_{24}H_{38}NO_2$ $[M + H]^+$ calc.: 372.2903; found: 372.2900.

IR (ATR, neat, cm^{-1}): 3299 (br), 3012 (m), 2962 (m), 2931 (m), 2873 (m), 1644 (s), 1584 (m), 1433 (m), 1067 (m), 704 (m).

Chemical synthesis of 19,20-EDP and 19,20-EDP-EA

Chemical synthesis of 19,20-EDP and 19,20-EDP-EA was performed using a two-step procedure. 0.1435 mmol DHA (NuChek Prep, Inc; catalog no.: U84A) was added to 2 ml of DCM in an 18 × 150 mm borosilicate test tube. *meta*-Chloroperoxybenzoic acid (0.2897 mmol) was added and pulse vortexed until dissolved. The resulting mixture was stirred and incubated for 1 h at 25 °C shielded from light. The nonspecific DHA-epoxidation was then added to a separatory funnel containing 15 ml DCM. About 20 ml H_2O was added and mixture inverted, followed by addition 10 ml 10% $NaHCO_3$ (w/v) and inversion. The layers were separated, and organic phase was collected. The extraction in the separatory funnel was repeated twice more with the addition of 20 ml DCM, and the collected organic phase was dried for separation on HPLC. The subsequent product was resuspended in EtOH and purified under reverse-phase HPLC as described later. 19,20-EDP-EA was next synthesized using a 1:40:40:40 M ratio of 19,20-EDP:1-ethyl-3-[3-dimethylaminopropyl]-carbodiimide hydrochloride:*N*-hydroxysuccinimide: ethanolamide on a rocker at room temperature for 18 h. Synthesis schematic can be viewed in Fig. S1.

Separation of epoxide regioisomers by HPLC

Extracted products of nonspecific DHA-epoxidation were separated under reverse-phase HPLC using the Waters Alliance e2695 HPLC system with the 2998 PDA detector. Purification was achieved using the SunFire C_{18} OBD 100 Å, 5 μm, 19 mm × 50 mm preparatory column (SunFire; catalog no.: 186002566). Solvents used were solvent A (95% H_2O, 4.9% ACN, 0.1% acetic acid [AcOH]) and solvent B (95% ACN, 4.9% H_2O, 0.1% AcOH). The flow rate was at 3 ml/min. The gradient is as follows: 0 min (50% A); 25 min (25% A); 40 min (25% A); 50 min (0% A); and 60 min (50% A). The resulting peak at 16 min was collected and verified by ESI TOF Mass Spectrometry in positive ion mode prior to use.

Synthesis of 19,20-DiHDPA and 19,20-DiHDPA-EA standards for LC–MS/MS analysis

Terminal epoxides of DHA and DHEA were synthesized and purified as described previously. The conversion of 19,20-EDP and 19,20-EDP-EA to their corresponding diol was accomplished as follows. Purified epoxides were solubilized in 2 ml ACN, and 2 ml of 1:1 glacial AcOH:water was added. The reaction was incubated at 45 °C for 1 h (Fig. S1). The resulting diols were purified by reverse-phase HPLC (Fig. S2). Successful synthesis of the standards was confirmed by high-resolution mass spectrometry. Peak at elution time 12 min was confirmed to be 19,20-DiHDPA-EA, and elution time at 23 min was 19,20-DiHDPA.

Data availability

All data generated during and/or analyzed during the current study are available on request by the first author or corresponding author.

Supporting information—This article contains supporting information.

Acknowledgments—We thank Dr Lucas Li at the Roy J. Carver Biotechnology Center for the assistance with LC–MS/MS. We also thank Dr David Sarlah for consulting on the organic synthesis.

Author contributions—J. S. K., A. J. S., and A. D. conceptualization; J. S. K., K. S.-D., A. J. S., and A. D. formal analysis; J. S. K., K. S.-D., A. J. S., and A. D. validation; J. S. K., K. S.-D., and T. B. investigation; A. J. S. and A. D. resources; J. S. K., K. S.-D., A. J. S., and A. D. data curation; J. S. K., A. J. S., and A. D. writing–original draft; J. S. K., K. S.-D., T. B., A. D., and A. J. S. writing–review & editing; J. S. K. and T. B. visualization; A. J. S. and A. D. supervision; A. J. S. and A. D. funding acquisition.

Funding and additional information—This research was funded in part by the National Multiple Sclerosis Society Pilot grant PP-1805-30908 and US Department of Agriculture—FIRE (grant no.: ILLU-538-932; to A. D. and A. J. S.), National Institutes of Health grant R03 RDA042365A (to A. D.), National Multiple Sclerosis Research grant (RG 1807-32053 to A. J. S.), Division of Nutritional Sciences Vision 20/20 grant (to A. D. and A. J. S.), and Division of Nutritional Sciences Margin of Excellence grants (to J. S. K.). J. S. K. was partially supported by the US Department of Agriculture National Institute of Food and Agriculture under the Nutrition and the Gut-Brain Axis: Implications for development and healthy aging grant (grant no.: 2019-38420-28973) to the Division of Nutritional Sciences at the University of Illinois.

Conflict of interest—The authors declare that they have no conflicts of interest with the contents of this article.

Abbreviations—The abbreviations used are: ACN, acetonitrile; AcOH, acetic acid; AEA, anandamide; 2-AG, 2-arachidonoylglycerol; CFA, complete Freund's adjuvant; CNS, central nervous system; DCM, dichloromethane; DHA, docosahexaenoic acid; DHEA, docosahexaenoyl ethanolamide; 19,20-DiHDPA-EA, 19,20-dihydroxydocosapentaenoylethanolamide; EAE, experimental autoimmune encephalomyelitis; eCB,

endocannabinoid; EDP-EA, epoxydocosahexaenoyl-ethanolamide; ESI, electrospray ionization; FBS, fetal bovine serum; IFNγ, interferon gamma; IL, interleukin; MFSD2A, major facilitator superfamily domain–containing protein 2; MOG, myelin oligodendrocyte glycoprotein; MS, multiple sclerosis; PLP, proteolipid protein; RR-EAE, relapse-remitting experimental autoimmune encephalomyelitis; TCR, T-cell receptor; TOF, time-of-flight.

References

1. Chaplin, D. D. (2010) Overview of the immune response. *J. Allergy Clin. Immunol.* **125**, S3–23
2. Laurent, P., Jolivel, V., Manicki, P., Chiu, L., Contin-Bordes, C., Truchetet, M. E., *et al.* (2017) Immune-mediated repair: a matter of plasticity. *Front. Immunol.* **8**, 454
3. Simopoulos, A. P. (2002) Omega-3 fatty acids in inflammation and autoimmune diseases. *J. Am. Coll. Nutr.* **21**, 495–505
4. Kromann, N., and Green, A. (1980) Epidemiological studies in the Upernavik district, Greenland. Incidence of some chronic diseases 1950-1974. *Acta Med. Scand.* **208**, 401–406
5. Devane, W. A., Hanus, L., Breuer, A., Pertwee, R. G., Stevenson, L. A., Griffin, G., *et al.* (1992) Isolation and structure of a brain constituent that binds to the cannabinoid receptor. *Science* **258**, 1946+
6. Felder, C. C., Briley, E. M., Axelrod, J., Simpson, J. T., Mackie, K., and Devane, W. A. (1993) Anandamide, an endogenous cannabimimetic eicosanoid, binds to the cloned human cannabinoid receptor and stimulates receptor-mediated signal transduction. *Proc. Natl. Acad. Sci. U. S. A.* **90**, 7656–7660
7. Sugiura, T., Kondo, S., Sukagawa, A., Nakane, S., Shinoda, A., Itoh, K., *et al.* (1995) 2-Arachidonoylgylcerol: a possible endogenous cannabinoid receptor ligand in brain. *Biochem. Biophys. Res. Commun.* **215**, 89–97
8. Di Marzo, V., Stella, N., and Zimmer, A. (2015) Endocannabinoid signalling and the deteriorating brain. *Nat. Rev. Neurosci.* **16**, 30–42
9. Kim, H. Y., and Spector, A. A. (2013) Synaptamide, endocannabinoid-like derivative of docosahexaenoic acid with cannabinoid-independent function. *Prostaglandins Leukot. Essent. Fatty Acids* **88**, 121–125
10. Bisogno, T., Delton-Vandenbroucke, I., Milone, A., Lagarde, M., and Di Marzo, V. (1999) Biosynthesis and inactivation of N-arachidonoylethanolamine (anandamide) and N-docosahexaenoylethanolamine in bovine retina. *Arch. Biochem. Biophys.* **370**, 300–307
11. Berger, A., Crozier, G., Bisogno, T., Cavaliere, P., Innis, S., and Di Marzo, V. (2001) Anandamide and diet: Inclusion of dietary arachidonate and docosahexaenoate leads to increased brain levels of the corresponding N-acylethanolamines in piglets. *Proc. Natl. Acad. Sci. U. S. A.* **98**, 6402–6406
12. Kim, H. Y., Spector, A. A., and Xiong, Z. M. (2011) A synaptogenic amide N-docosahexaenoylethanolamide promotes hippocampal development. *Prostaglandins Other Lipid Med.* **96**, 114–120
13. Kim, H. Y., Moon, H. S., Cao, D., Lee, J., Kevala, K., Jun, S. B., *et al.* (2011) N-Docosahexaenoylethanolamide promotes development of hippocampal neurons. *Biochem. J.* **435**, 327–336
14. Park, T., Chen, H., Kevala, K., Lee, J. W., and Kim, H. Y. (2016) N-Docosahexaenoylethanolamine ameliorates LPS-induced neuroinflammation *via* cAMP/PKA-dependent signaling. *J. Neuroinflam.* **13**, 284
15. Wang, Y., Plastina, P., Vincken, J. P., Jansen, R., Balvers, M., Ten Klooster, J. P., *et al.* (2017) N-docosahexaenoyl dopamine, an endocannabinoid-like conjugate of dopamine and the n-3 fatty acid docosahexaenoic acid, attenuates lipopolysaccharide-induced activation of microglia and macrophages *via* COX-2. *ACS Chem. Neurosci.* **8**, 548–557
16. Czepiel, J., Gdula-Argasińska, J., Biesiada, G., Bystrowska, B., Jurczyszyn, A., Perucki, W., *et al.* (2019) Fatty acids and selected endocannabinoids content in cerebrospinal fluids from patients with neuroinfections. *Metab. Brain Dis.* **34**, 331–339
17. Georgieva, M., Wei, Y., Dumitrascuta, M., Pertwee, R., Finnerup, N. B., and Huang, W. (2019) Fatty acid suppression of glial activation prevents central neuropathic pain after spinal cord injury. *Pain* **160**, 2724–2742
18. Balvers, M. G., Verhoeckx, K. C., Plastina, P., Wortelboer, H. M., Meijerink, J., and Witkamp, R. F. (2010) Docosahexaenoic acid and eicosapentaenoic acid are converted by 3T3-L1 adipocytes to N-acyl ethanolamines with anti-inflammatory properties. *Biochim. Biophys. Acta* **1801**, 1107–1114
19. Meijerink, J., Plastina, P., Vincken, J. P., Poland, M., Attya, M., Balvers, M., *et al.* (2011) The ethanolamide metabolite of DHA, docosahexaenoylethanolamine, shows immunomodulating effects in mouse peritoneal and RAW264.7 macrophages: Evidence for a new link between fish oil and inflammation. *Br. J. Nutr.* **105**, 1798–1807
20. Meijerink, J., Poland, M., Balvers, M. G., Plastina, P., Lute, C., Dwarkasing, J., *et al.* (2015) Inhibition of COX-2-mediated eicosanoid production plays a major role in the anti-inflammatory effects of the endocannabinoid N-docosahexaenoylethanolamine (DHEA) in macrophages. *Br. J. Pharmacol.* **172**, 24–37
21. Yang, R., Fredman, G., Krishnamoorthy, S., Agrawal, N., Irimia, D., Piomelli, D., *et al.* (2011) Decoding functional metabolomics with docosahexaenoyl ethanolamide (DHEA) identifies novel bioactive signals. *J. Biol. Chem.* **286**, 31532–31541
22. McDougle, D. R., Watson, J. E., Abdeen, A. A., Adili, R., Caputo, M. P., Krapf, J. E., *et al.* (2017) Anti-inflammatory omega-3 endocannabinoid epoxides. *Proc. Natl. Acad. Sci. U. S. A.* **114**, E6034–E6043
23. Goldenberg, M. M. (2012) Multiple sclerosis review. *P T* **37**, 175–184
24. Compston, A., and Coles, A. (2008) Multiple sclerosis. *Lancet* **372**, 1502–1517
25. Disanto, G., Berlanga, A. J., Handel, A. E., Para, A. E., Burrell, A. M., Fries, A., *et al.* (2010) Heterogeneity in multiple sclerosis: scratching the surface of a complex disease. *Autoimmune Dis.* **2011**, 932351
26. Lucchinetti, C., Brück, W., Parisi, J., Scheithauer, B., Rodriguez, M., and Lassmann, H. (2000) Heterogeneity of multiple sclerosis lesions: Implications for the pathogenesis of demyelination. *Ann. Neurol.* **47**, 707–717
27. Lassmann, H., Brück, W., and Lucchinetti, C. (2001) Heterogeneity of multiple sclerosis pathogenesis: Implications for diagnosis and therapy. *Trends Mol. Med.* **7**, 115–121
28. Hauser, S. L., Waubant, E., Arnold, D. L., Vollmer, T., Antel, J., Fox, R. J., *et al.* (2008) B-cell depletion with rituximab in relapsing-remitting multiple sclerosis. *N. Engl. J. Med.* **358**, 676–688
29. Kivisäkk, P., Healy, B. C., Viglietta, V., Quintana, F. J., Hootstein, M. A., Weiner, H. L., *et al.* (2009) Natalizumab treatment is associated with peripheral sequestration of proinflammatory T cells. *Neurology* **72**, 1922–1930
30. Polman, C. H., O'Connor, P. W., Havrdova, E., Hutchinson, M., Kappos, L., Miller, D. H., *et al.* (2006) A randomized, placebo-controlled trial of natalizumab for relapsing multiple sclerosis. *N. Engl. J. Med.* **354**, 899–910
31. McCandless, E. E., Piccio, L., Woerner, B. M., Schmidt, R. E., Rubin, J. B., Cross, A. H., *et al.* (2008) Pathological expression of CXCL12 at the blood-brain barrier correlates with severity of multiple sclerosis. *Am. J. Pathol.* **172**, 799–808
32. Dutta, R., and Trapp, B. D. (2007) Pathogenesis of axonal and neuronal damage in multiple sclerosis. *Neurology* **68**, S22–S31
33. Criste, G., Trapp, B., and Dutta, R. (2014) Axonal loss in multiple sclerosis: causes and mechanisms. *Handb Clin. Neurol.* **122**, 101–113
34. Lauer, K. (1997) Diet and multiple sclerosis. *Neurology* **49**, S55–61
35. Buoite Stella, A., Gortan Cappellari, G., Barazzoni, R., and Zanetti, M. (2018) Update on the impact of omega 3 fatty acids on inflammation, insulin resistance and sarcopenia: a review. *Int. J. Mol. Sci.* **19**. https://doi.org/10.3390/ijms19010218
36. Calder, P. C. (2013) Omega-3 polyunsaturated fatty acids and inflammatory processes: Nutrition or pharmacology? *Br. J. Clin. Pharmacol.* **75**, 645–662
37. Dyall, S. C., and Michael-Titus, A. T. (2008) Neurological benefits of omega-3 fatty acids. *Neuromol. Med.* **10**, 219–235
38. Siegert, E., Paul, F., Rothe, M., and Weylandt, K. H. (2017) The effect of omega-3 fatty acids on central nervous system remyelination in fat-1 mice. *BMC Neurosci.* **18**, 19
39. Wysoczański, T., Sokoła-Wysoczańska, E., Pękala, J., Lochyński, S., Czyż, K., Bodkowski, R., *et al.* (2016) Omega-3 fatty acids and their role in central nervous system - a review. *Curr. Med. Chem.* **23**, 816–831

40. Bates, D. (1989) Lipids and multiple sclerosis. *Biochem. Soc. Trans.* **17**, 289–291
41. Hoare, S., Lithander, F., van der Mei, I., Ponsonby, A. L., Lucas, R., and Group, A. I. (2016) Higher intake of omega-3 polyunsaturated fatty acids is associated with a decreased risk of a first clinical diagnosis of central nervous system demyelination: results from the Ausimmune Study. *Mult. Scler.* **22**, 884–892
42. Arévalo-Martín, A., Vela, J. M., Molina-Holgado, E., Borrell, J., and Guaza, C. (2003) Therapeutic action of cannabinoids in a murine model of multiple sclerosis. *J. Neurosci.* **23**, 2511–2516
43. Arevalo-Martin, A., Molina-Holgado, E., and Guaza, C. (2012) A CB_1/CB_2 receptor agonist, WIN 55,212-2, exerts its therapeutic effect in a viral autoimmune model of multiple sclerosis by restoring self-tolerance to myelin. *Neuropharmacology* **63**, 385–393
44. Pryce, G., Ahmed, Z., Hankey, D. J., Jackson, S. J., Croxford, J. L., Pocock, J. M., *et al.* (2003) Cannabinoids inhibit neurodegeneration in models of multiple sclerosis. *Brain* **126**, 2191–2202
45. Benito, C., Romero, J. P., Tolón, R. M., Clemente, D., Docagne, F., Hillard, C. J., *et al.* (2007) Cannabinoid CB1 and CB2 receptors and fatty acid amide hydrolase are specific markers of plaque cell subtypes in human multiple sclerosis. *J. Neurosci.* **27**, 2396–2402
46. Tabula Muris Consortium, Overall coordination, Logistical coordination, Organ collection and processing, Library preparation and sequencing, Computational data analysis, Cell type annotation, Writing group, Supplemental text writing group, Principal investigators (2018) Single-cell transcriptomics of 20 mouse organs creates a Tabula Muris. *Nature* **562**, 367–372
47. Zajicek, J., Fox, P., Sanders, H., Wright, D., Vickery, J., Nunn, A., *et al.* (2003) Cannabinoids for treatment of spasticity and other symptoms related to multiple sclerosis (CAMS study): multicentre randomised placebo-controlled trial. *Lancet* **362**, 1517–1526
48. Zajicek, J. P., Sanders, H. P., Wright, D. E., Vickery, P. J., Ingram, W. M., Reilly, S. M., *et al.* (2005) Cannabinoids in multiple sclerosis (CAMS) study: safety and efficacy data for 12 months follow up. *J. Neurol. Neurosurg. Psych.* **76**, 1664–1669
49. Zajicek, J. P., Hobart, J. C., Slade, A., Barnes, D., Mattison, P. G., and Group, M. R. (2012) Multiple sclerosis and extract of cannabis: results of the MUSEC trial. *J. Neurol. Neurosurg. Psych.* **83**, 1125–1132
50. Acharya, N., Penukonda, S., Shcheglova, T., Hagymasi, A. T., Basu, S., and Srivastava, P. K. (2017) Endocannabinoid system acts as a regulator of immune homeostasis in the gut. *Proc. Natl. Acad. Sci. U. S. A.* **114**, 5005–5010
51. Watson, J. E., Kim, J. S., and Das, A. (2019) Emerging class of omega-3 fatty acid endocannabinoids & their derivatives. *Prostaglandins Other Lipid Med.* **143**, 106337
52. Fletcher, J. M., Lalor, S. J., Sweeney, C. M., Tubridy, N., and Mills, K. H. (2010) T cells in multiple sclerosis and experimental autoimmune encephalomyelitis. *Clin. Exp. Immunol.* **162**, 1–11
53. Bettelli, E., Pagany, M., Weiner, H. L., Linington, C., Sobel, R. A., and Kuchroo, V. K. (2003) Myelin oligodendrocyte glycoprotein-specific T cell receptor transgenic mice develop spontaneous autoimmune optic neuritis. *J. Exp. Med.* **197**, 1073–1081
54. Robinson, R. H., Meissler, J. J., Fan, X., Yu, D., Adler, M. W., and Eisenstein, T. K. (2015) A CB2-selective cannabinoid suppresses T-cell activities and increases tregs and IL-10. *J. Neuroimmune Pharmacol.* **10**, 318–332
55. Centonze, D., Bari, M., Rossi, S., Prosperetti, C., Furlan, R., Fezza, F., *et al.* (2007) The endocannabinoid system is dysregulated in multiple sclerosis and in experimental autoimmune encephalomyelitis. *Brain* **130**, 2543–2553
56. Kong, W., Yen, J. H., and Ganea, D. (2011) Docosahexaenoic acid prevents dendritic cell maturation, inhibits antigen-specific Th1/Th17 differentiation and suppresses experimental autoimmune encephalomyelitis. *Brain Behav. Immun.* **25**, 872–882
57. Eisenstein, T. K., and Meissler, J. J. (2015) Effects of cannabinoids on T-cell function and resistance to infection. *J. Neuroimmune Pharmacol.* **10**, 204–216
58. Jaudszus, A., Gruen, M., Watzl, B., Ness, C., Roth, A., Lochner, A., *et al.* (2013) Evaluation of suppressive and pro-resolving effects of EPA and DHA in human primary monocytes and T-helper cells. *J. Lipid Res.* **54**, 923–935
59. Centonze, D., Battistini, L., and Maccarrone, M. (2008) The endocannabinoid system in peripheral lymphocytes as a mirror of Neuroinflammatory diseases. *Curr. Pharm. Des.* **14**. https://doi.org/10.2174/138161208785740018
60. Hillard, C. J., Weinlander, K. M., and Stuhr, K. L. (2012) Contributions of endocannabinoid signaling to psychiatric disorders in humans: genetic and biochemical evidence. *Neuroscience* **204**, 207–229
61. Boorman, E., Zajkowska, Z., Ahmed, R., Pariante, C. M., and Zunszain, P. A. (2016) Crosstalk between endocannabinoid and immune systems: a potential dysregulation in depression? *Psychopharmacology (Berl)* **233**, 1591–1604
62. Pan, Y., Morris, E. R., Scanlon, M. J., Marriott, P. J., Porter, C. J. H., and Nicolazzo, J. A. (2018) Dietary docosahexaenoic acid supplementation enhances expression of fatty acid-binding protein 5 at the blood-brain barrier and brain docosahexaenoic acid levels. *J. Neurochem.* **146**, 186–197
63. Lacombe, R. J. S., Chouinard-Watkins, R., and Bazinet, R. P. (2018) Brain docosahexaenoic acid uptake and metabolism. *Mol. Aspects Med.* **64**, 109–134
64. Nguyen, L. N., Ma, D., Shui, G., Wong, P., Cazenave-Gassiot, A., Zhang, X., *et al.* (2014) Mfsd2a is a transporter for the essential omega-3 fatty acid docosahexaenoic acid. *Nature* **509**, 503–506
65. Pifferi, F., Laurent, B., and Plourde, M. (2021) Lipid transport and metabolism at the blood-brain interface: implications in health and disease. *Front. Physiol.* **12**, 645646. https://doi.org/10.3389/fphys.2021.645646
66. Chan, J. P., Wong, B. H., Chin, C. F., Galam, D. L. A., Foo, J. C., Wong, L. C., *et al.* (2018) The lysolipid transporter Mfsd2a regulates lipogenesis in the developing brain. *PLoS Biol.* **16**, e2006443. https://doi.org/10.1371/journal.pbio.2006443
67. Davis, J. N., Courtney, C. L., Superak, H., and Taylor, D. K. (2014) Behavioral, clinical and pathological effects of multiple daily intraperitoneal injections on female mice. *Lab. Anim. (Ny)* **43**, 131–139
68. Lewis, E. J. (2013) Omega-3 fatty acid supplementation and cardiovascular disease events. *JAMA* **309**, 27
69. Tian, J., Geng, F., Gao, F., Chen, Y. H., Liu, J. H., Wu, J. L., *et al.* (2017) Down-regulation of neuregulin1/ErbB4 signaling in the Hippocampus is critical for learning and memory. *Mol. Neurobiol.* **54**, 3976–3987
70. Baker, D., Gerritsen, W., Rundle, J., and Amor, S. (2011) Critical appraisal of animal models of multiple sclerosis. *Mult. Scler.* **17**, 647–657
71. Zamvil, S., Nelson, P., Trotter, J., Mitchell, D., Knobler, R., Fritz, R., *et al.* (1985) T-cell clones specific for myelin basic protein induce chronic relapsing paralysis and demyelination. *Nature* **317**, 355–358
72. Whitham, R. H., Bourdette, D. N., Hashim, G. A., Herndon, R. M., Ilg, R. C., Vandenbark, A. A., *et al.* (1991) Lymphocytes from SJL/J mice immunized with spinal cord respond selectively to a peptide of proteolipid protein and transfer relapsing demyelinating experimental autoimmune encephalomyelitis. *J. Immunol.* **146**, 101–107
73. Maresz, K., Pryce, G., Ponomarev, E. D., Marsicano, G., Croxford, J. L., Shriver, L. P., *et al.* (2007) Direct suppression of CNS autoimmune inflammation *via* the cannabinoid receptor CB1 on neurons and CB2 on autoreactive T cells. *Nat. Med.* **13**, 492–497
74. Kong, W., Li, H., Tuma, R. F., and Ganea, D. (2014) Selective CB2 receptor activation ameliorates EAE by reducing Th17 differentiation and immune cell accumulation in the CNS. *Cell Immunol.* **287**, 1–17
75. Ashton, J. C., and Glass, M. (2007) The cannabinoid CB2 receptor as a target for inflammation-dependent neurodegeneration. *Curr. Neuropharmacol.* **5**, 73–80
76. Cassano, T., Calcagnini, S., Pace, L., De Marco, F., Romano, A., and Gaetani, S. (2017) Cannabinoid receptor 2 signaling in neurodegenerative disorders: from pathogenesis to a promising therapeutic target. *Front. Neurosci.* **11**, 30
77. Thapa, D., Cairns, E. A., Szczesniak, A. M., Kulkarni, P. M., Straiker, A. J., Thakur, G. A., *et al.* (2020) Allosteric cannabinoid receptor 1 (CB1) ligands reduce ocular pain and inflammation. *Molecules* **25**. https://doi.org/10.3390/molecules25020417

78. Chiurchiù, V., Leuti, A., Dalli, J., Jacobsson, A., Battistini, L., Maccarrone, M., *et al.* (2016) Proresolving lipid mediators resolvin D1, resolvin D2, and maresin 1 are critical in modulating T cell responses. *Sci. Transl. Med.* **8**, 353ra111
79. Dyall, S. C., Balas, L., Bazan, N. G., Brenna, J. T., Chiang, N., da Costa Souza, F., *et al.* (2022) Polyunsaturated fatty acids and fatty acid-derived lipid mediators: recent advances in the understanding of their biosynthesis, structures, and functions. *Prog. Lipid Res.* **86**, 101165
80. Kooij, G., Troletti, C. D., Leuti, A., Norris, P. C., Riley, I., Albanese, M., *et al.* (2020) Specialized pro-resolving lipid mediators are differentially altered in peripheral blood of patients with multiple sclerosis and attenuate monocyte and blood-brain barrier dysfunction. *Haematologica* **105**, 2056–2070
81. Sánchez-Fernández, A., Zandee, S., Mastrogiovanni, M., Charabati, M., Rubbo, H., Prat, A., *et al.* (2022) Administration of Maresin-1 ameliorates the physiopathology of experimental autoimmune encephalomyelitis. *J. Neuroinflam.* **19**, 27
82. Francos-Quijorna, I., Santos-Nogueira, E., Gronert, K., Sullivan, A. B., Kopp, M. A., Brommer, B., *et al.* (2017) Maresin 1 promotes inflammatory resolution, neuroprotection, and functional neurological recovery after spinal cord injury. *J. Neurosci.* **37**, 11731–11743
83. Stromnes, I. M., and Goverman, J. M. (2006) Active induction of experimental allergic encephalomyelitis. *Nat. Protoc.* **1**, 1810–1819